Energy 66 (2014) 82–89

Contents lists available at ScienceDirect

Energy

journal homepage: www.elsevier.com/locate/energy

Plasmatron gasification of biomass lignocellulosic waste materials derived from municipal solid waste

Je-Lueng Shie [a], [*], Li-Xun Chen [a], Kae-Long Lin [a], Ching-Yuan Chang [b]

[a] Department of Environmental Engineering, National I-Lan University, 260 I-Lan, Taiwan
[b] Graduate Institute of Environmental Engineering, Nation Taiwan University, 106 Taipei Taiwan

ARTICLE INFO

Article history:
Received 28 June 2012
Received in revised form
16 October 2013
Accepted 19 December 2013
Available online 15 January 2014

Keywords:
Syngas
Plasmatron
Gasification
Municipal solid waste
Steam mechanical heat treatment
Refuse solid biomass (RSB)

ABSTRACT

The aim of this work is to study the feasibility and operational performance of plasmatron (plasma torch) gasification of municipal solid waste mixed with raw wood (MSW/RW) derived from the pretreatment of Steam Mechanical Heat Treatment (SMHT), as the target material (MRM). A 10 kW plasmatron reactor is used for gasification of the MRM. The production of syngas (CO and H_2) is the major component, and almost 90% of the gaseous products appear in 2 min of reaction time, with relatively high reaction rates. The syngas yield is between 88.59 and 91.84 vol%, and the recovery mass ratio of syngas from MRM is 45.19 down to 27.18 wt% with and without steam with the energy yields of 59.07–111.89%. The concentrations of gaseous products from the continuous feeding of 200 g/h are stable and higher than the average concentrations of the batch feeding of 10 g. The residue from the plasmatron gasification with steam is between 0 and 4.52 wt%, with the inorganic components converted into non-leachable vitrified lava, which is non-hazardous. The steam methane reforming reaction, hydrogasification reaction and Boudouard reaction all contribute to the increase in the syngas yield. It is proved that MSW can be completely converted into bioenergy using SMHT, followed by plasmatron gasification.

© 2013 Elsevier Ltd. All rights reserved.

1. Introduction

Energy from waste (EFW) is a sustainable and environmental friendly waste disposal and can provide better waste disposal of municipal solid waste (MSW). The transformation of waste into energy can be efficiently achieved by applying thermochemical techniques, such as torrefaction, partial oxidation, pyrolysis, gasification and synthesis [1–9]. Papageorgiou et al. [10] found that the greenhouse gas (GHG) impact highly depends on the MSW treatments and the end market of the solid recovery fuel (SRF) or refuse derived fuel (RDF). However, the quality and stability of SRF or RDF are not high enough for them to serve as supplement fuels or to derive power from combustion, especially for long distance transportation and extended storage time [9]. If the MSW is treated by steam mechanical heat treatment (MHT), the fiber and flock can be easily separated as SRF or RDF [11]. Garg et al. [12] reported that SRF has a Higher Heating Value (HHV) of about 15–18 MJ kg^{-1} (or 3585–4302 kcal/kg), and that it is a suitable co-combustion fuel for coal power plants or cement kilns.

The pyrolysis/gasification of solid waste to produce syngas offers an alternative to energy supplied by fossil fuels. Because syngas essentially contains molecular hydrogen and carbon monoxide, it has the potential for use as a high-quality fuel. Moreover, after purification, it becomes an important source of hydrogen, which is important in the context of fuel cell technology [13]. However, the purification or separation of syngas is another technology which should be developed and advanced. It will be easier to use the syngas as fuel for the power generation or cogeneration. Notably, the use of plasmatron pyrolysis or gasification offers unique advantages for solid waste conversion, such as providing high temperatures and heating rates, in comparison to conventional pyrolysis or gasification methods [7–9]. A suitable pretreatment process enhances the pyrolysis or gasification effects. Erlach et al. [14] pointed out that pre-treating the biomass with hydrothermal carbonization (HTC) produces a coal-like substance, biocoal, which is potentially better suited for entrained flow gasification than raw biomass. Byun et al. [15] developed a gasification/vitrification unit for the direct treatment of municipal solid waste (MSW), with a capacity of 10 tons/day, using an integrated furnace equipped with two nontransferred thermal plasma torches. It was successfully demonstrated that this process converted MSW into innocuous slag, with much lower levels of environmental air pollutant emissions and the syngas having a utility value as energy sources

---

[*] Corresponding author. Tel./fax: +886 39353563.
E-mail address: jlshie@niu.edu.tw (J.-L. Shie).

0360-5442/$ – see front matter © 2013 Elsevier Ltd. All rights reserved.
http://dx.doi.org/10.1016/j.energy.2013.12.042

(287 N m^3/MSW-ton for H_2 and 395 N m^3/MSW-ton for CO), using 1.14 MWh/MSW-ton of electricity (thermal plasma torch (0.817 MWh/MSW-ton) + utilities (0.322 MWh/MSW-ton)) and 7.37 N m^3/MSW-ton of liquefied petroleum gas [15].

In this study, the treatment of MSW mixed with raw wood (MSW/RW) via Steam Mechanical Heat Treatment (SMHT), using a thermal plasmatron reactor as the heat source, was examined. The waste, in the view of sustainable material management (SMM), is regarded as the used material. The ultimate goal of SMM is total recycling and reuse without waste, thereby achieving a green environment. In keeping with this goal, the MHT of MSW/RW focuses on the feasibility of total recovery and reutilization. SMHT is one of the alternatives for the pretreatment of MSW/RW before its further reutilization. SMHT, sometimes referred to as wet torrefaction, is an artificial coalification process which takes place in hot pressurized water between 175 and 250 °C. It involves hydrolysis, decarboxylation, dehydratization, condensation and aromatization reactions [16]. SMHT is one of the alternatives for the pretreatment of municipal solid waste (MSW) using waste steam effluent from incinerator plants before its further separation and reutilization. For the heat recycling consideration, the waste steam effluent is derived from the off-stream steam from co-generator in incinerator plant. After SMHT, the lignocellulosic in MSW becomes refuse-derived biomass (RDB), and the properties of MSW are significantly changed. For example, the mass decreases while the volume density increases. The autoclaving serves as a pre-treatment step of MHT for the better separation yielding floc/fibre or RDF of good quality. The quality of derived floc/fibre depends on the properties of the MSW [17]. The biomass of MSW/RW from SMHT (MRM), which is compost-like and primary RDF or bio-char, becomes suitable for torrefaction/pyrolysis or gasification. The main objective of this study was to assess the plasmatron gasification of MRM with different temperatures and to examine the effects of the operation parameters on the performance, with the aim of providing product distribution with different contents. The gasification was performed using a plasmatron system in a nitrogen atmosphere with a 10 kW power capacity with steam contents. The residual materials and non-condensable gases were collected and analyzed using an elemental analyzer, gas analytical instruments and gas chromatography analyzers with thermal conductivity detectors (GC–TCD).

2. Material and methods

2.1. Materials

The biomass used in this study was MRM. The MRM was taken from the MSW/RW after the pretreatment of SMHT, which was performed by a fertilizer company in I-Lan, Taiwan. The sample of MRM was dried in a recycling ventilation drier for 24 h at 378 K before use. For a comparison of the effect of steam content, the water flow rate (circulated by a 378 K heating tape for steam production) was adjusted to 1 and 3 mL min^{-1} and injected into the plasmatron reactor. The results of the proximate analysis of MRM were 57.21, 4.12, and 38.67 wt% for moisture, ash and combustibles, respectively. As shown in Table 1, the contents of C, H, N, S and Cl of dry MRM were 53.13, 7.34, 1.49, 0.37 and 0.12 wt%, respectively, and the higher heating value (HHV) and lower heating value (LHV) of dry MRM were 9.71 and 7.59 MJ kg^{-1}, respectively.

2.2. Plasmatron operational procedure

A pilot-scale apparatus was used, and the experimental procedures for the plasmatron steam gasification were similar to those in previous studies [6,7], as shown in Fig. 1. A 10 kW plasmatron was used for the gasification process. For batch feeding, a sample of known mass of about 10 g was placed on the sample apparatus for feeding the sample material; then a 10 g sample flowed through the sample apparatus at 3 min intervals. The flow rate of carrier gas N_2 (99.99%) (Q_N) was adjusted to the desired value, i.e., 10 L min^{-1} at 101.3 kPa (1 atm) and 293 K, and was controlled by a rotameter. The power supply control unit (chopper) (Taiwan Plasma Corp.) for the plasmatron reactor was set at 2.59–4.68 kW (P_L) for temperatures (T) ranging from 573 to 873 K, respectively. For the analysis of gas products, a Gas Chromatograph GC–TCD (Thermo Scientific FOCUS GC) with a Supelco packing column (60/80 carbonxen-1000, 15 ft long, 2.1 mm i.d.) was used. The operation conditions of the Gas Chromatograph GC–TCD were set as follows: injector temperature 453 K, detector temperature 513 K, column temperature (following the sampling injection) held at 513 K for 10 min, helium carrier gas flow rate of 30 mL min^{-1} for A and B columns and a sample volume of 2 mL. Several duplicate experimental runs were performed in order to verify the values.

Table 1
Elemental analysis, calorific value and BET surface area of MRM and solid residues derived from plasmatron gasification at various temperatures and steam flow rates.

	Target temperature ± 20 (K)	573 K		773 K		873 K		873 K		873 K	
	Water flow rate for steam generation (mL min^{-1})	0		0		0		1		3	
	Dry MRM[a]										
Element											
C	53.13	65.86[b]	17.69[c]	54.66[b]	9.93[c]	56.27[b]	7.96[c]	41.25[b]	1.86[c]	33.27[b]	2.66[c]
H	7.34	0.79[b]	0.21[c]	0.47[b]	0.09[c]	0.47[b]	0.07[c]	1.28[b]	0.06[c]	0.92[b]	0.07[c]
N	1.49	1.95[b]	0.52[c]	1.62[b]	0.30[c]	3.92[b]	0.55[c]	1.25[b]	0.06[c]	2.12[b]	0.17[c]
S	0.37	0.10[b]	0.03[c]	0.09[b]	0.02[c]	0.39[b]	0.06[c]	0.01[b]	0[c]	0.00[b]	0[c]
C/H ratio (wt/wt)	7.24	83.37[b]		116.30[b]		119.72[b]		32.23[b]		36.16[b]	
Mass ratio[d]			26.87		18.46		14.15		4.52		–
Calorific value (MJ kg^{-1})											
HHV[e]	9.71	6.38		7.53		8.47		0.76		1.13	
LHV[f]	7.59	4.27		8.47		6.35		–		–	
BET surface area (m^2 g^{-1})	–	19.49		34.85		65.18		70.70		81.21	

[a] MRM: municipal solid waste mixed with raw wood (MSW/RW) after Steam Mechanical Heat Treatment (SMHT) (blade type) (MSW:RW = 8:1).
[b] Based on mass of residue.
[c] Based on original mass of raw MRM.
[d] Mass ratio of residue to raw MRM.
[e] Higher heating value of dry basis.
[f] Lower heating value of dry basis.

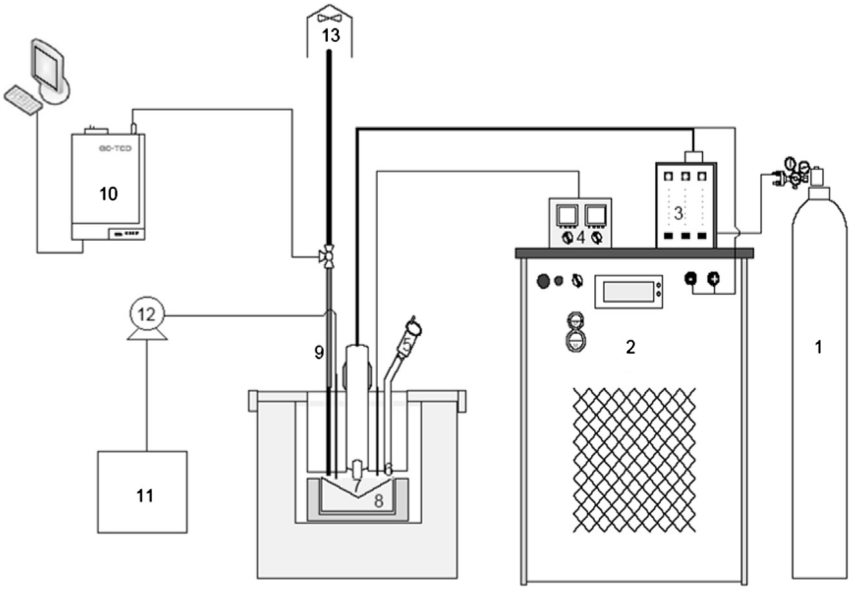

Fig. 1. Schematic diagram of apparatus for the 10 kW plasmatron. 1. Nitrogen cylinder. 2. Power supply chopper and cooling system. 3. Gas flow rate controller. 4. Thermo detector. 5. Sample input apparatus. 6. Sample. 7. Plasma torch and reactor. 8. Crucible. 9. Circulating water pipe and outlet line. 10. Gas detectors and analytical instruments. 11. Steam generator.

3. Results and discussion

3.1. Characteristics of residues for plasmatron steam gasification of MRM

3.1.1. Elemental analysis

The elemental analysis of MRM and its residues at different temperatures and steam conditions for plasmatron gasification are presented in Table 1. As indicated, carbon (C) was the major element in the solid residues (excluding oxygen). It was clear that the hydrogen, sulfur and nitrogen were insignificant and could be neglected. The C/H ratio in the solid residues showed increases from that of the raw material (7.24) to 83.37, 116.3 and 119.72 at 573, 773 and 873 K, respectively, without steam injection. However, the C/H ratio decreased to 32.23 and 36.16 at 873 K with steam injection of 1 and 3 mL min^{-3} water flow rates, respectively. The rate of escape of H was larger than that of C in this range. With the steam injection at 873 K, the rate of escape of C showed an obvious increase. Notably, C decreased drastically from 53.13 wt% to 7.96 and 1.86 wt% at 873 K without steam and at 873 K with 1 mL min^{-1} steam, respectively. Almost all of the elements (excluding carbon and oxygen) were near zero (0–0.55 wt%, relative to raw MRM). The weight percentage of residue was 14.15 wt% for a reaction temperature of 873 K without steam injection. With steam injection, the weight percentage decreased to 4.52 and near zero wt% at 873 K with 1 and 3 mL min^{-1} water flow rates, respectively, which implied that steam dramatically enhanced the reaction. Therefore, the residue at this high temperature or input power with steam was lava-like.

3.1.2. Calorific value analysis

Parr calorimeter (Oxygen bomb plain jacket calorimeter, model 1341; Ignition unit 115/50/60, model 2901EB; Digital thermometer assy 6775, Model A360C; Parr instrument Co., Moline, IL) was employed to measure the calorific value of sample, according to ASTM D2015. The highest HHV of MRM residue after plasmatron gasification was 8.47 and 1.13 MJ kg^{-1} at 873 K without and with 3 mL min^{-1} steam injection, respectively (Table 1). The HHV of MRM residue with steam injection was almost a tenth of that without steam injection. It was reasonable that almost all the C and H escaped after the steam injection. Furthermore, the H_L of MRM residue with steam injection was near zero, as the water flow rate enhanced the carbon gasification by steam and the entire residue converted to lava.

3.1.3. BET surface analysis

The BET surface areas of residue from the plasmatron gasification were calculated using the BET equation, as listed in Table 1. After plasmatron gasification, the BET surface area increased from 19.49 m^2 g^{-1} at 573 K to 65.48 m^2 g^{-1} at 873 K without steam. The gasification of MRM by plasmatron with steam increased the BET surface area of residue to 4.17 times from 573 K to 873 K. After steam injection, the larger BET surface area of 81.21 m^2 g^{-1} at 873 K with a 3 mL min^{-1} water flow rate resulting from steam gasification was believed to be due to the activation by steam and higher density of plasma. Therefore, the residue formed by plasma gasification could be reused as active carbon for resource recovery at the optimum condition of steam injection.

3.2. Effects of temperature in the instantaneous gaseous products

In this study, gaseous samples were collected via the instantaneous sampling method and detected using GC–TCD. The instantaneous concentrations of CO [CO], H_2 [H_2], CH_4 [CH_4] and CO_2 [CO_2] in gaseous products at 573, 773 and 873 K and reaction times (t_{rsf}, = reaction time of the solid sample in the furnace after loading) are shown in Fig. 2(a)–(d), respectively. As shown in Fig. 2(a), the maximum instantaneous concentrations and the corresponding t_{rsf} of H_2 occurred at 1) 92,528 ppmv for 573 K at 1.25 min, 2) 143,486 ppmv for 773 K at 1.25 min and 3) 178,627 ppmv for 873 K, respectively, at 0.75 min with 0.5 min sampling intervals. Fig. 2(b) shows that the maximum instantaneous [CO] occurred at 0.75 min with [CO] of 110,772 ppmv for 573 K, 127,531 ppmv for 773 K and 167,364 ppmv for 873 K, respectively. CO and H_2 (syngas) were the major components of the gaseous products, with a temperature of 873 K yielding a maximum concentration of 345,991 ppmv at a relatively high reaction rate. The maximum concentration of syngas increased with the increase of temperature. The formation of H_2

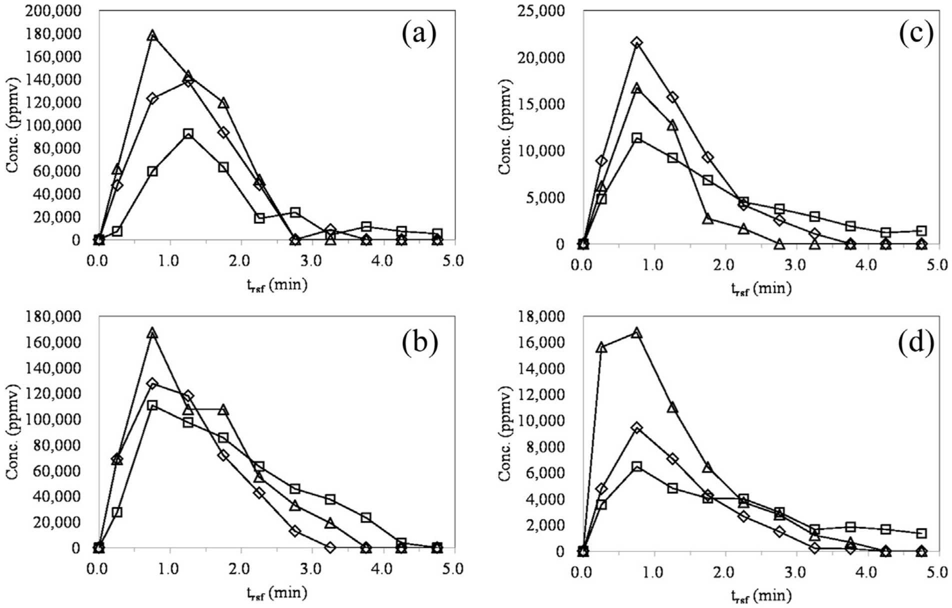

Fig. 2. Instantaneous concentrations in gaseous products from the gasification of MRM using plasmatron. □, ◇, △: 573, 773, 873 K. t_{rsf}: reaction time of solid sample in furnace after loading. (a) H_2, (b) CO, (c) CH_4, (d) CO_2.

was more vigorous than the conversion of C to CO, as indicated in Fig. 1(a) and (b), with [H_2] higher than [CO] at 873 and 773 K. Almost 90% of the gaseous products appeared within a 2 min reaction time. Therefore, compared to conventional thermal gasification, the reaction time of 2 min was considerably shorter. Thus, the elevated heating rate of the plasmatron allowed the reaction to reach maximum product concentration quickly. The plasmatron could be characterized with its elevated energy density, which allowed for faster treatment of solid waste, such as MRM, than with conventional gasification methods.

As Fig. 2(c) shows, the maximum instantaneous concentrations of CH_4 occurred at 11,397 ppmv for 573 K, 21,610 ppmv for 773 K and 16,739 ppmv for 873 K at 0.75 min, respectively, with 0.5 min sampling intervals. It was clear that the maximum concentration of CH_4 occurred at 773 K. However, the maximum concentration of CH_4 for these three temperatures was still far lower than those of the other gaseous products. The reason may be due to the low limitation of thermodynamic of methane formation as well as relative to other products. From Fig. 2(d), the maximum instantaneous concentrations of CO_2 appear at 6486 ppmv for 573 K, 9442 ppmv for 773 K and 16,759 ppmv for 873 K at 0.75 min, respectively, with 0.5 min sampling intervals. The concentration of CO_2 increased with the increase of the reaction temperature. Notably, high temperatures enhanced the formation of CO_2. This syngas is mainly composed of carbon monoxide (CO) and hydrogen (H_2) with low quantities of carbon dioxide (CO_2), water (H_2O), methane (CH_4), hydrogen sulfide (H_2S), ammonia (NH_3), and under certain conditions, solid carbon (C), nitrogen (N_2), argon (Ar) and some tar traces. Nitrogen and argon coming from the use of air as the reactant or are due to their use as plasma gas. Shie et al. [5] pointed out that other pollutants appeared in the effluent gases, such as SO_2, NOx and HCl, and that their maximum instantaneous concentration was between 2.61 and 11.42 ppmv for the plasma pyrolysis of sunflower-oil cake. Almost no tar was found in the plasma pyrolysis or gasification conditions. The gas quality allows direct application to fuel. Therefore, an analysis of these pollutants was not part of this study. As regards the suppression of pollutants emitted and the reduction of the power consumption, the reaction temperature could be controlled at certain temperatures, specifically, below 973 K [5–7]. Therefore, we chose 873 K as the constant temperature for testing the effects of steam on the plasmatron gasification of MRM.

3.3. Effects of steam for the instantaneous gaseous products

Fig. 3(a) and (b) shows the instantaneous concentrations of CO and H_2, respectively, in gaseous products from the gasification of MRM using a plasmatron reactor under steam flow. Relative to the plasmatron gasification of MRM without steam, as shown in Fig. 3(a), the maximum instantaneous concentration and the corresponding t_{rsf} of H_2 with steam occurred at 244,144 and 183,879 ppmv at 0.75 and 1.25 min with 0.5 min sampling intervals at a water flow rate of 3 and 1 mL min^{-1}, respectively. The maximum concentration of H_2 increased with the increase of the water flow rate. As Fig. 3(b) shows, the maximum instantaneous concentration of CO occurred with [CO] of 169,420 ppmv at 0.75 min and a water flow rate of 3 mL min^{-1}. Relative to the maximum concentrations of 167,364 and 150,589 ppmv at 0 and 1 mL min^{-1} water flow rates, respectively, the increased concentration of CO was not obvious with steam injection. However, the maximum concentration of syngas (sum of CO and H_2) of 413,564 ppmv with a 3 mL min^{-1} steam flow rate was higher than the 345,991 ppmv without steam. The 19.53% increase of syngas was the result of the increase of H_2.

As Fig. 3(c) shows, the maximum instantaneous concentration of CH_4 at 873 K with steam occurred at 18,276 ppmv and 0.25 min with 0.5 min sampling intervals at a 3 mL min^{-1} water flow rate. After a reaction time of 3 min, the concentration of CH_4 could be ignored. However, the maximum concentration of CH_4 for the steam condition was similar to that without steam at 873 K. This may have been due to the simultaneous occurrence of a steam methane reforming reaction ($CH_4 + 2H_2O \rightarrow CO + 3H_2$) and a hydrogasification ($C + H_2 \rightarrow CH_4$) reaction. After 1.25 min reaction time, it was reasonable that the concentration of CO and H_2 was increased by the steam methane reforming reaction. As shown in Fig. 3(d), the maximum instantaneous concentration of CO_2 with steam appeared at 23,587 ppmv and 1.75 min with a 0.5 min sampling interval at a 3 mL min^{-1} water flow rate. It was clear that

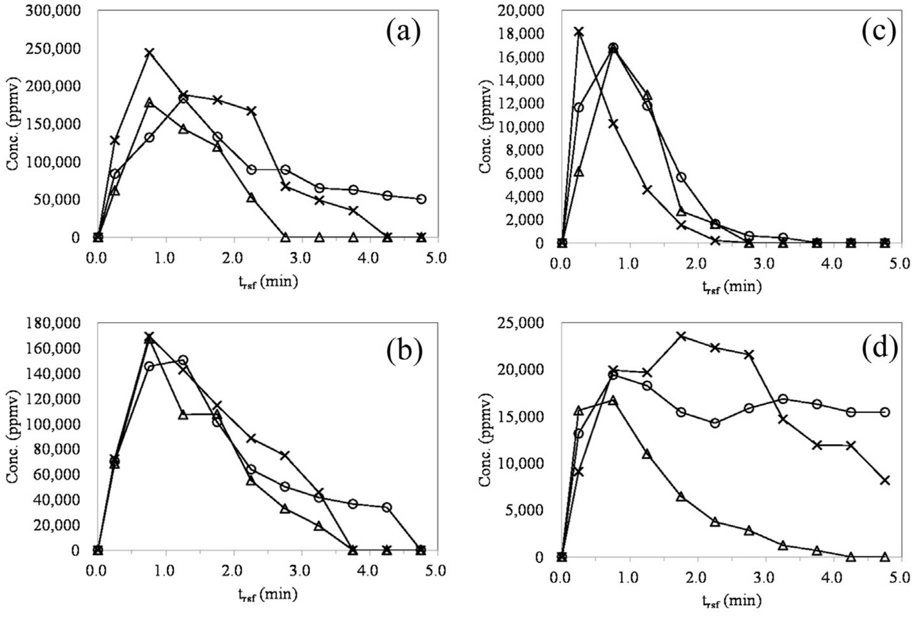

Fig. 3. Instantaneous concentrations in gaseous products from the steam plasmatron gasification of MRM using plasmatron. △, ○, ×: 0, 1, 3 mL min^{-1}. t_{rsf}: As specified in Fig. 2. Reaction temperature = 873 K. (a) H_2, (b) CO, (c) CH_4, (d) CO_2.

the presence of steam enhanced the continuous release of CO_2. Notably, the concentrations of CO_2 with the steam condition were also higher than those cases without steam after 0.75 min reaction time. This case was similar to that of H_2 and CO production and the result of the water–gas shift reaction ($CO + H_2O \rightarrow CO_2 + H_2$).

3.4. Effects of temperature, loading and steam in the accumulated gaseous products

The accumulated masses of gaseous products from three reaction temperatures of MRM with and without steam are shown in Table 2. Table 2 also shows the accumulated mass and volume fractions of the effluent gaseous products relative to total mass and volume of gaseous products (CO, H_2, CH_4 and CO_2) (excluding the carrier gas N_2) in wt% and vol%; the yields and ratios of the accumulated mass of syngas and CO_2; and the residues in the reactor for different conditions of gasification after the cooling process. The maximum accumulated volume fractions of the syngas ratio (mass of syngas/sum mass of CO, H_2, CH_4 and CO_2) without steam increased from 89.87 vol% at 573 K to 91.84 vol% at 873 K with the increase in temperature. CO and H_2 (syngas) were the major components in the gas products, with the temperature yielding the summary maximum accumulated syngas mass yield (=sum mass of syngas/dry basis of MRM) at 873 K, with 33.98 wt% without steam and 45.15 wt% with 3 mL min^{-1} steam for an MRM mass of about 10 g. The lowest total residue ratio (=sum mass of residue/dry basis of MRM) was also at 873 K with 14.15 wt%. The evident increase of the production mass of H_2 and decreased mass of CH_4 with the increase of steam may have been due to the decomposition of H_2O and CH_4 supplying the hydrogen source at 873 K. This was understandable because the steam injection increased the total mass of input raw material (MRM and steam). Similar tendencies also appeared in the accumulated masses of CO and CO_2; this was due to the decomposition of water, and so additional oxygen. Regarding the production of greenhouse gases, the accumulated vol% of CO_2 showed an obvious change with steam injection, as shown from the value of the CO_2 yield (mass of CO_2/dry sample mass × 100%) of 5.19 wt% without steam to 14.13 wt% with steam injection of 3 mL min^{-1} at 873 K. As regards another greenhouse gas, CH_4, the accumulated vol% of CH_4 decreased from 3.3 vol% without steam to 1.78 vol% with steam injection of 3 mL min^{-1} at 873 K. This may have been due to the increase of the steam methane reforming reaction ($CH_4 + 2H_2O \rightarrow CO + 3H_2$), the promotion reactions of the Boudouard reaction ($CO_2 + C \rightarrow 2CO$) and the inhibition of the methane production reaction ($C + 2H_2 \rightarrow CH_4$), which enhanced the production of syngas [6,7]. The heating value of syngas and energy yield of syngas in Table 2 without steam increased from 48.73 kJ and 50.14% at 573 K to 64.27 kJ and 65.46% at 873 K, respectively, with the increase in temperature. The energy yield of syngas was larger than 100% in steam cases because the steam injection increased the total mass of syngas.

3.5. Effects of continuous loading of MRM on gaseous products

In order to have comparable information with the batch reaction, continuous feeding was performed with a feeding rate of 200 g/h at 873 K without steam. The resulting gaseous products are shown in Fig. 4(a) and (b). The average concentrations of batch feeding of H_2, CO, CH_4 and CO_2 were 94,291, 78,300, 8060 and 5980 ppmv, respectively. After the reaction times of 5 min for H_2 and CO (Fig. 4(a)) and 7.5 min for CH_4 and CO_2 (Fig. 4(b)), the concentrations were stable and higher than the average concentrations for batch feeding, attributable to both the longer reaction time and a more complete reaction. The final concentrations of H_2, CO, CH_4 and CO_2 in the continuous feeding were about 225,000, 165,000, 20,500 and 11,500 ppmv, respectively, under the feeding rate of 200 g/h at 873 K without steam. Therefore, the sum concentrations of all gases were higher than 18.7% for batch feeding and 42.2% for continuous feeding. The obtained information proved the possibility of continuous operation, which will be useful for the rational design of plasmatron gasification systems. However, there is a vitally important concern of the use of electric energy, because it can substantially raise the operating cost of the use of plasma torch. In order to overcome parts of this problem, the need of electric energy for plasma torch may be supplied partly from the power generated via the use of product of syngas.

Table 2
Accumulated masses of gaseous products and effluent gasses from the gasification of MRM using a plasmatron reactor with/without steam (excluding of H_2O, NOx, SOx, and N_2).[a]

Target temperature (K)	Dry sample mass (g)	Water flow rate (mL min^{-1})	CO		H_2		CH_4		CO_2		Total gas mass		Syngas ratio[e]		Syngas yield[f] (wt%)	CO_2 yield[g] (wt%)	Heating value of syngas (kJ)	Energy yield of syngas[h] (%)
			wt%[b]	vol%[c]	wt%[b]	vol%[c]	wt%[b]	vol%[c]	wt%[b]	vol%[c]	g	wt%[d]	wt%	vol%				
573 ± 20	10.01 (0.02)[i]	0	79.91 (0.50)	53.41 (3.10)	3.90 (1.06)	36.46 (4.01)	4.37 (0.48)	5.11 (0.16)	11.83 (1.73)	5.03 (1.07)	3.57 (0.25)	35.66 (2.58)	83.81 (1.25)	89.87 (0.91)	29.88 (1.72)	4.22 (0.89)	48.73 (57.42)[j]	50.14 (59.07)[k]
773 ± 20	10.04 (0.08)	0	79.02 (3.01)	44.84 (2.79)	5.70 (0.23)	45.32 (2.01)	6.84 (2.01)	6.79 (1.84)	8.43 (0.76)	3.05 (0.20)	3.22 (0.48)	32.07 (5.07)	84.72 (2.78)	90.16 (2.05)	27.18 (3.41)	2.71 (0.67)	51.95 (64.21)[j]	53.29 (65.87)[k]
873 ± 20	10.11 (0.13)	0	78.54 (1.46)	46.62 (6.72)	5.44 (1.70)	45.22 (8.14)	3.18 (0.47)	3.30 (0.89)	12.84 (0.24)	4.85 (0.52)	4.09 (0.95)	40.45 (8.93)	83.98 (0.24)	91.84 (1.42)	33.98 (7.41)	5.19 (1.05)	64.27 (71.51)[j]	65.46 (72.84)[k]
873 ± 20	10.17 (0.01)	1	66.85 (1.67)	38.10 (1.45)	6.33 (0.25)	50.49 (1.30)	2.64 (0.34)	2.64 (0.37)	24.18 (1.76)	8.77 (0.52)	5.98 (0.36)	58.80 (3.59)	73.18 (1.42)	88.59 (0.15)	43.04 (3.48)	14.22 (0.19)	94.5 (103.29)[j]	95.7 (104.6)[k]
873 ± 20	9.96	3	67.00	36.51	6.99	53.34	1.86	1.78	24.15	8.37	6.08	61.04	73.99	89.85	45.15	14.73	101.91 (108.21)[j]	105.38 (111.89)[k]

[a] VRM: raw waste vegetables mixed with raw wood (RWV/RW) from Steam Mechanical Heat Treatment (SMHT) (RWV:RW = 5:1).
[b] wt% = gas mass/sum mass of CO, H_2, CH_4 and CO_2.
[c] vol% = gas mole/sum moles of CO, H_2, CH_4 and CO_2.
[d] Total gas yield = total gas mass/dry sample mass × 100%, wt%.
[e] Syngas ratio = mass of syngas/sum mass of CO, H_2, CH_4 and CO_2.
[f] Syngas yield = mass of syngas/dry sample mass × 100%.
[g] CO_2 yield = mass of CO_2/dry sample mass × 100%.
[h] Heating value of syngas/high heating value of sample × 100%.
[i] Numbers in parentheses are standard derivations (σ_n).
[j] Heating value of CO + H_2 + CH_4.
[k] Energy yield of all fuel gases (CO + H_2 + CH_4).

3.6. Energy efficiency evaluations

Conventional technologies for energy recovery from waste are based on incineration, pyrolysis or gasification processes. Incineration is already a well-established and stable process and electrical energy can be drawn with efficiencies below 30%. For the energy consumption of plasmatron, Tendler et al. [13] proposed that the energy productions of syngas for steam thermodynamic cycle (about 35% efficiency) and combined cycle (about 52% efficiency) were 5.35 and 7.96 MJ kg^{-1} from wood, 5.06 and 7.52 MJ kg^{-1} from RDF, and 10.37 and 15.27 MJ kg^{-1} from car tyres, respectively. Comparison with the energy consumptions of processing the wood, RDF and car tyres for plasma torch gasification of 3.6, 3.82 and 6.66 MJ kg^{-1}, respectively, the energy stored in syngas are all higher than that energy consumption from the operation of plasmatron. From the energy life-cycle assessment (ELCA), the energy input required in the transportation and pretreatment stages is the greatest component of energy use. The pre-treatment includes drying, crushing and briquetting. For the convenience required for feeding feedstock into the thermal reactor, crushing and briquetting are needed in the production of RDF. It is evident the energy consumption of dryers used for torrefaction purposes is far larger than that of others [9]. In general, the main goal of drying is to decrease the moisture content of solid materials below a certain limit, especial for the MRM after the SMTH process. However, all energy return on investment (EROI) values of this assessed plasmatron system in previous ELCA study

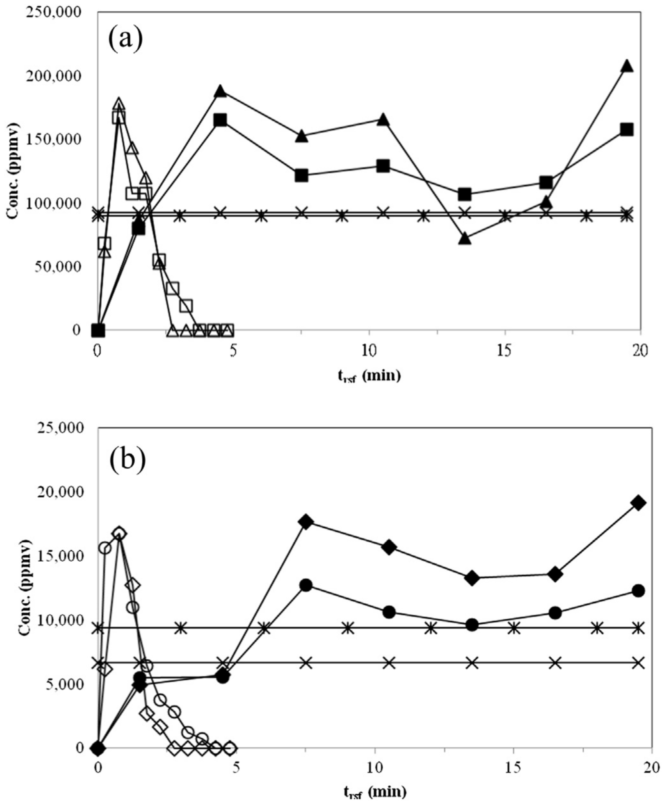

Fig. 4. The concentrations in gaseous products from the gasification of MRM using plasmatron at 873 K with the continuous feeding of 200 g/h and batch feeding of 10 g. (a) △: H_2 at batch operation, ▲: H_2 at continuous operation, ×: average concentration of H_2 at batch operation, □: CO at batch operation, ■: CO at continuous operation, *: average concentration of CO at batch operation. (b) ◇: CH_4 at batch operation, ◆: CH_4 at continuous operation, ×: average concentration of CH_4 at batch operation, ○: CO_2 at batch operation, ●: CO_2 at continuous operation, *: average concentration of CO_2 at batch operation. t_{rsf}: As specified in Fig. 2. Reaction temperature = 873 K.

are far larger than 1 [9]. EROI here is defined by the ratio of gaining useful energy. Every energy input is taken into the process and converted to produce energy in one or more forms [18]. The higher the EROI, the more renewable the biofuel is. Falcucci et al. [19] addressed an integrated MCFC-plasma gasifier energy system. This model has been further integrated in a numerical tool designed to predict the performances of a novel waste-to-energy system based on the integration of a plasma torch gasification unit, an MCFC power unit and a steam turbine. The numerical results point out that an integrated power system featuring a 1 MW MCFC would produce a net electrical power of 782 kW with an electric efficiency of about 30.3% by using 720 kg/h of RDF as fuel. The efficiency would rise up to 36% by employing more efficient steam turbines in larger power systems. This efficiency is higher than those reached by conventional technologies based on RDF incineration (i.e. net efficiencies on the order of 14–25% [20–22]) and is comparable with the efficiencies of the integrated systems based on combined cycle and SOFC stacks, previously analyzed by the authors [20,23]. In order to evaluate the reliability and environmental sustainability of plasma technology for energy recovery from solid wastes, an integrated plasma gasification combined cycle (IPGCC) power plant has been investigated and its performance has been evaluated by Minutillo et al. [20]. The results pointed out that, considering the torch power consumption and the maximum size of commercially available plasma torches (2.5 MW), six torches have to be installed in the IPGCC power plant as well as the gas turbine fed with syngas produces 26.6 MW and the steam power section produces 18 MW. In comparison with conventional technologies in the waste to energy recovery, electric power is produced with higher efficiency (31% vs. 20% of RDF conventional incineration power plant) and low harmful pollutants (i.e. dioxins and furans are not produced) [20]. For the efficiency of plasma gasification of wood residues, the advantages of plasma by comparison with existing thermochemical processes are in the high heating value gases, process control and the lower energy consumption per unit of output. Rutberg et al. [24] pointed out that it is possible to obtain 4.6–4.8 MJ of electricity (net of electricity input) and 9.1–9.3 MJ of thermal energy when using wood with average elemental composition and with an LHV energy content of 13.9 MJ from 1 kg of 20% moisture wood, when using a combined Brayton and Steam cycle generating plant. Experimental data from an air plasma gasification plant using alternating current (AC) plasma torches was integrated with a thermodynamic model showing that the chemical energy in the produced syngas was 13.8–14.3 MJ kg^{-1} with a power input of 2.2–3.3 MJ kg^{-1}. By now, the power of plasmatrons can vary from ~10 kW to ~6 MW, and efficiency achieves 70–94% [24]. Zhang et al. [25] also addressed that the plasma power using in MSW treatment is about 2.88 MJ kg^{-1} MSW in their study cases. Zhang et al. [26] evaluated the plasma flow supplies heat for gasification in the PGM process. The amount of plasma heat is characterized by plasma energy ratio (PER). It was found that both gasification temperature and pyrolysis temperature increase linear with PER. This is easy to understand since increasing PER enhance the average temperature of feeding air, and increases the heat supply for gasification and pyrolysis. When PER increases from 0.098 to 0.137, the syngas yield increases from 0.96 to 1.08 N m^3/kg MSW. At the same time the syngas LHV varies from 7.32 to 9.31 MJ/N m^3. It seems the positive effects of PER provides a possible method for not only solving the tar problem, but also increase the syngas yield and quality. Hong et al. [27] also evaluated the cold gas efficiency of a coal gasification investigation using an atmospheric-pressure pure steam torch plasma which was generated by making use of 2.45 GHz microwave energy. The plasma power of about 4 kW was applied. The calorific power of synthetic gas and the calorific power of the coal are 8 and 14.6 kW, respectively. Therefore, the cold gas efficiency is $\eta = 8$ kW/(14.6 kW + 4 kW) = 0.43. The difference between the calorific powers of the coal and synthetic gas is 14.6 − 8 = 6.6 kW, which may be disappeared due to radiation and conduction loss of the reaction chamber being hot and owing to convective loss through the discharge of hot gas with average temperature of 2000 K. Therefore, the energy efficiency is also taken consideration in this study.

4. Conclusions

In this study, a 10 kW plasmatron reactor was used for gasification of the biomass lignocellulosic waste materials derived from municipal solid waste. Almost 90% of the gaseous products appeared within a 2 min reaction time with relatively high reaction rates. The production of syngas was the major component of the gas products. Syngas increased with the increase of temperature without steam. Nevertheless, the maximum concentration of H_2 increased with the increase of steam. The increase of the production mass of H_2 and decreased mass of CH_4 with the increase of steam may have been due to the decomposition of H_2O and CH_4 to supply the hydrogen source, and attributable to the steam methane reforming reaction, hydrogasification, the promotion reactions of the Boudouard reaction, and the inhibition of the methane production reaction at the same time. The obvious increase of CO_2 after the injection of steam was due to the water–gas shift reaction. The inorganic components were converted into non-leachable and non-hazardous vitrified lava. All the information obtained in this study will prove useful for the rational design and proper operation of plasmatron gasification systems in the treatment of MSW.

Acknowledgments

We express our sincere thanks to the National Science Council of Taiwan for their generous financial support, under contract No. NSC 101-3113-E-002-012.

Nomenclature

Abbreviation

EFW	energy from waste
EROI	energy return on investment
GC–TCD	gas chromatography–thermal conductivity detector
GHG	greenhouse gas
HHV	higher heating value
HTC	hydrothermal carbonization
LHV	lower heating value
MHT	mechanical heat treatment
MRM	biomass of MSW/RW from SMHT
MSW	municipal solid waste
MSW/RW	municipal solid waste mixed with raw wood
RDB	refuse-derived biomass
RDF	refuse derived fuel
RSB	refuse solid biomass
RW	raw wood
SMHT	steam mechanical heat treatment
SMM	sustainable material management
SRF	solid recovery fuel

Symbols

P	power (W)
T	temperature (K)

References

[1] Wang MJ, Huang YF, Chiueh PT, Kuan WH, Lo SL. Microwave-induced torrefaction of rice husk and sugarcane residues. Energy 2012;37:177–84.

[2] Fischer B, Pigneri A. Potential for electrification from biomass gasification in Vanuatu. Energy 2011;36:1640–51.

[3] Shie JL, Chang CY, Lin JP, Wu CH, Lee DJ, Chang CF. Kinetics of the oxidative thermal treatment of oil sludge at low heating rates. Energy Fuels 2004;18:1272–81.

[4] Shie JL, Lin JP, Chang CY, Wu CH, Shih SM, Lee DJ. Pyrolysis of oil sludge with additives of catalytic solid wastes. J Anal Appl Pyrol 2004;71:695–707.

[5] Shie JL, Chang CY, Tu WK, Tang YC, Liao JK, Tzeng CC, et al. Major products obtained from plasma torch pyrolysis of sunflower-oil cake. Energy Fuels 2008;22:75–82.

[6] Shie JL, Tsou FJ, Lin KL, Chang CY. Bioenergy and products from thermal pyrolysis of rice straw using plasma torch. Bioresour Technol 2010;101:761–8.

[7] Shie JL, Tsou FJ, Lin KL. Steam plasmatron gasification of distillers grains residue from ethanol production. Bioresour Technol 2010;101:5571–7.

[8] Shie JL, Chang CY, Tzeng CC, Hung PY, Chang CC, Chiang SW, et al. Water-enhanced reforming of syngas to fuels and chemicals in a batch reactor. Sustain Environ Res 2010;20:181–7.

[9] Shie JL, Chang CY, Chen CS, Shaw DG, Chen YH, Kuan WH, et al. Energy life cycle assessment of rice straw bio-energy derived from potential gasification technologies. Bioresour Technol 2011;102:6735–41.

[10] Papageorgiou A, Barton JR, Karagiannidis A. Assessment of the greenhouse effect impact of technologies used for energy recovery from municipal waste: a case for England. J Environ Manage 2009;90:2999–3012.

[11] Shie JL, Chen LX, Lin KL, Li YS, Ma HK, Chang CY. Plasmatron gasification of raw waste vegetables from steam mechanical heat treatment. Fresenius Environ Bull 2012;21(8c):2499–505.

[12] Garg A, Smith R, Hill D, Simms N, Pollard S. Wastes as co-fuels: the policy framework for solid recovered fuel (SRF) in Europe, with UK implications. Environ Sci Technol 2007;41:4868–74.

[13] Tendler M, Rutberg P, van Oost G. Plasma based waste treatment and energy production. Plasma Phys and Control Fusion 2005;47. A219A230.

[14] Erlach B, Harder B, Tsatsaronis G. Combined hydrothermal carbonization and gasification of biomass with carbon capture. Energy 2012:1–10.

[15] Byun Y, Namkung W, Cho M, Chung JW, Kim YS, Lee JH, et al. Demonstration of thermal plasma gasification/vitrification for municipal solid waste treatment. Environ Sci Technol 2010;44(17):6680–4.

[16] Funke A, Ziegler F. Hydrothermal carbonization of biomass: a summary and discussion of chemical mechanisms for process engineering. Biofuels Bioprod Biorefin 2010;4(2):160–77.

[17] Hung ZS, Chang CC, Ho Chang CF, Wang YC, Chang CY, Ji DR, et al. Autoclaving of waste plastic-free papers for resource recovery and reutilization. Fresenius Environ Bull 2012;21(8c):2486–93.

[18] Irfan MF, Arami-Niya A, Chakrabarti MH, Mohd W, Daud AW, Usman MR. Kinetics of gasification of coal, biomass and their blends in air (N_2/O_2) and different oxy-fuel (O_2/CO_2) atmospheres. Energy 2012;37:665–72.

[19] Falcucci G, Jannelli E, Minutillo M, Ubertini S, Han J, Yoon SP, et al. Integrated numerical and experimental study of a MCFC-plasma gasifier energy system. Appl Energy 2012;97:734–42.

[20] Minutillo M, Perna A, Di Bona D. Modelling and performance analysis of an integrated plasma gasification combined cycle (IPGCC) power plant. Energy Convers Manage 2009;50:2837–42.

[21] Vitasari CR, Jurascik M, Ptasinski KJ. Exergy analysis of biomass-to-synthetic natural gas (SNG) process via indirect gasification of various biomass feedstock. Energy 2011;36:3825–37.

[22] Galvarino J, Balcazar C, Dias RA, Balestieri JAP. Analysis of hybrid waste-to-energy for medium-sized cities. Energy 2013:1–14. http://dx.doi.org/10.1016/j.energy.2013.02.003.

[23] Isaksson J, Pettersson K, Mahmoudkhani M, Åsblad A, Berntsson T. Integration of biomass gasification with a scandinavian mechanical pulp and paper mill – consequences for mass and energy balances and global CO_2 emissions. Energy 2012;44:420–8.

[24] Rutberg PG, Bratsev AN, Kuznetsov VA, Popov VE, Ufimtsev AA, Shtengel SV. On efficiency of plasma gasification of wood residues. Biomass Bioenergy 2011;35:495–504.

[25] Zhang Q, Dor L, Fenigshtein D, Yang W, Blasiak W. Gasification of municipal solid waste in the plasma gasification melting process. Appl Energy 2012;90:106–12.

[26] Zhang Q, Dor L, Zhang L, Yang W, Blasiak W. Performance analysis of municipal solid waste gasification with steam in a plasma gasification melting reactor. Appl Energy 2012;98:219–29.

[27] Hong YC, Lee SJ, Shin DH, Kim YJ, Lee BJ, Cho SY, et al. Syngas production from gasification of brown coal in a microwave torch plasma. Energy 2012;47:36–40.